Eur Radiol (2013) 23:3077–3086
DOI 10.1007/s00330-013-2906-y

MAGNETIC RESONANCE

Diffusion-weighted magnetic resonance imaging: new perspectives in the diagnostic pathway of non-complicated acute pyelonephritis

Agostino De Pascale · Giorgina Barbara Piccoli · Sandro Massimo Priola · Daniela Rognone · Valentina Consiglio · Irene Garetto · Laura Rizzo · Andrea Veltri

Received: 31 January 2013 / Revised: 22 April 2013 / Accepted: 2 May 2013 / Published online: 8 June 2013

Abstract
Objectives The diagnosis of acute pyelonephritis (APN) requires demonstration of parenchymal involvement. When no predisposing conditions are found, non-complicated APN is suspected and CT or MRI should be performed. Diffusion-weighted (DW) MRI might be useful, quicker and cheaper than the standard gadolinium-enhanced (GE) MRI. The aim of this study is to compare DW-MRI with GE-MRI to test its diagnostic accuracy in APN.
Methods Of 318 consecutive patients hospitalised for APN, 279 underwent MRI. Four hundred and fourteen MR studies (first test and follow-up examinations) were gathered and data were processed using Diffusion Analysis software. DW-MRI has been compared with GE-MRI for evaluating diagnostic agreement.
Results Two hundred and forty-four patients were diagnosed as having APN; 35 were negative. One hundred and sixty-three APN cases were considered non-complicated and selected for the study. Among the 414 MR examinations, comparing DW-MRI with GE-MRI, positive correlation was found in 258 cases, negative in 133. There were 14 false-negatives and 9 false-positives. DW-MRI achieved sensitivity 95.2 %, specificity 94.9 %, positive predictive value 96.9 %, negative predictive value 92.3 % and accuracy 94.6 %.
Conclusions DW-MRI is reliable for diagnosing non-complicated APN. The high diagnostic agreement between DW-MRI and GE-MRI offers new perspectives in diagnostic management, enabling diagnosis of non-complicated APN without using ionising radiation or contrast media.
Key Points
- *The diagnosis of acute pyelonephritis (APN) requires demonstration of renal involvement.*
- *Hitherto magnetic resonance imaging required gadolinium enhancement (GE-MRI) to establish this diagnosis.*
- *But diagnostic agreement between diffusion-weighted and GE-MRI offers new diagnostic opportunities.*
- *Quantification of ADC values can help diagnose and monitor APN.*
- *DW-MRI avoids ionising radiation and paramagnetic contrast medium administration.*

Keywords Acute pyelonephritis · Urinary tract infections · Gadolinium-enhanced magnetic resonance imaging · Diffusion-weighted magnetic resonance imaging · Apparent diffusion coefficient

A. De Pascale · S. M. Priola · D. Rognone · L. Rizzo
Department of Diagnostic Imaging, San Luigi Gonzaga Hospital, University of Torino, Orbassano, Torino, Italy

G. B. Piccoli · V. Consiglio
Department of Clinical and Biological Sciences, San Luigi Gonzaga Hospital, University of Torino, Orbassano Torino, Italy

I. Garetto · A. Veltri (✉)
Department of Oncology, San Luigi Gonzaga Hospital, University of Torino, Orbassano, Torino, Italy
e-mail: andrea.veltri@unito.it

I. Garetto
e-mail: irgaretto@yahoo.it

Introduction

In the USA acute pyelonephritis (APN) has an incidence as high as 250,000 cases per year, mostly in young women, and necessitates 200,000 hospitalisations every year [1–3]. There are very few data on the overall incidence of APN in Europe, being influenced by the type of sanitary system and the hospitalisation policy; however, based on a previous

surveillance on the referral area of our university hospital, the gross incidence of hospitalised APN cases can be estimated as about 26.5 new cases per year per 100,000 inhabitants.

APN develops when uropathogens ascend to the kidneys from faecal flora; rarely it is caused by seeding of the kidneys by bacteraemia.

According to the British Medical Research Council Bacteriuria Committee [4], the definition of APN is clinical, based on a classic tetrad of high fever, costovertebral angle tenderness, signs or symptoms of lower urinary tract infection (UTI) (leucocytosis, pyuria) and positive urinary cultures. As this definition does not discriminate between upper UTI with or without renal parenchymal involvement, other authors follow a "pathological" criterion, based upon the demonstration of kidney involvement by imaging techniques [5].

A general consensus is reached for the definition of "complicated" versus "non-complicated" APN [6–8]. "Complicated" refers to the presence of systemic (any factor affecting the immune response, including diabetes, collagen disease, neoplasia, chemotherapy, HIV positivity, neuromuscular disease, haemoglobinopathies) or anatomical (any factor causing obstruction, including active stone disease, prostatic hypertrophy, kidney malformations, reflux nephropathy, polycystic kidney disease and indwelling catheters) predisposing factors. "Non-complicated" refers to their absence.

Moreover the most significant elements in the recent literature regarding APN are the revised guidelines for treatment. In their paper Gupta et al. [9] underline the need for differentiating between patients requiring hospitalisation and those who do not. Only imaging data can distinguish between upper UTI with and without parenchymal involvement.

In view of its low sensitivity for the presence of parenchymal lesions [10] and the high sensitivity for obstructive lesions, conventional ultrasound is used to identify the presence of anatomical predisposing factors.

In cases in which there is a clinical suspicion of APN, in which no predisposing condition is found at ultrasound, non-complicated APN should be suspected and a second-line imaging test has to be performed. Computed tomography (CT) or magnetic resonance imaging (MRI) examination allows precise definition of the inflammatory areas and evidence of abscesses [11–13]. As patients with non-complicated APN are mostly women of childbearing age, MR might be chosen as the preferred imaging technique and CT should be performed only in the case of contraindications or logistical problems (long wait before the availability of an MRI) [14].

MRI, using a parallel imaging technique acquisition, is able to perform dynamic enhanced studies, with diagnostic accuracy superimposable onto CT [15]. It does not use ionising radiation and it is equipped with considerable contrast resolution. Between sequences performed in a basal setting, diffusion-weighted magnetic resonance imaging (DW-MRI) has recently gained particular interest [16]. It is realisable by analysing the spin dephasing and signal loss caused by random motion along magnetic field gradients. The apparent diffusion coefficient (ADC), as a quantitative parameter calculated from the DW-MRI, combines the effects of capillary perfusion and water diffusion in the intracellular extravascular space.

The kidneys are very challenging organs for DW-MRI. The development of echo-planar imaging (EPI), high gradient amplitudes, multichannel coils and parallel imaging have been helpful in increasing the applications of DW sequences. In particular, the introduction of parallel imaging, such as sensitivity encoding (SENSE), which allowed reduction in the echo-train length (TE) and the K-space filling time, led to considerably less motion artefacts at image acquisition, thus enabling high-quality DW images of the body to be acquired. Hence, DWI might be useful in differentiating APN, with the advantage of lower costs and execution times than gadolinium-enhanced MRI (GE-MRI).

The aim of our study was to evaluate diagnostic agreement between DWI and GE-MRI (the "gold standard" test), to estimate the capability of DW-MRI in the evaluation of non-complicated APN and to demonstrate its potential reliability in the diagnostic pathway.

Materials and methods

Selection of patients

All consecutive patients admitted to our hospital with the diagnosis of APN in the period January 2007-September 2009, and hospitalised from the Emergency Department (ED) to the Emergency Medicine, Urology and Nephrology or Internal Medicine wards, were considered for the study. All patients were referred to the Radiology Unit during hospitalisation and were followed at least until clinical and radiological healing (with a 3- to 6-week interval, according to the severity of the disease). Clinical data were gathered prospectively, whereas the MRI studies have been analysed retrospectively.

The clinical suspicion of APN was made by the ED physicians, based on the presence of at least one of the three main symptoms (fever, costovertebral angle tenderness or pain, recent or present UTI) and at least one sign of systemic infection (high white blood cells or C-reactive protein [CRP]). The diagnosis of present or recent UTI was based on urinalysis or the clinical history. All patients with a clinical picture suggestive of APN underwent abdominal ultrasound, whenever possible in the ED, and were hospitalised. In patients hospitalised for fever of unknown origin, in which the diagnosis was made during hospitalisation, ultrasound was performed subsequently.

The following general data were collected, to differentiate complicated versus non-complicated APN: age, sex, previous UTI, previous history of pyelonephritis, previous stone disease. Patients with kidney stones were not included. At referral, the following clinical data were collected: fever, costovertebral angle-tenderness, lower UTI symptoms, other symptoms; antibiotic therapy within the last 72 h; other therapies.

Laboratory data were obtained using standard laboratory methods. The following data, obtained in the ED at hospitalisation, were considered: serum creatinine, blood cell counts, CRP, urinary cultures, haemocultures and the results of dipstick urinalysis were also recorded when available. In the presence of systemic predisposing factors and/or of anatomical predisposing factors detected by ultrasound, the APN was considered as complicated and the patients were not included in the study.

By definition, diagnosis was made by a second-line imaging technique. MRI was performed in 279 patients (264 females and 15 males) with a median age of 35 years (16–77 years). Thirty-nine remaining patients (including two pregnant patients) did not undergo MRI at our Unit or were subjected to CT or, rarely, underwent only ultrasound. Selection of patients to submit for MRI at our Service was usually carried out by our nephrologists.

Out of 279 patients who underwent MRI, diagnosis of APN was made in 244, while in 35 cases the investigation was negative.

In keeping with the diagnosis of non-complicated APN, all patients (163) were female, with a median age of 32 years but a wide age range (16–72 years), with a normal genito-urinary tract.

Eighty-one patients with complicated APN, diagnosed on the basis of gender (15 male patients with benign prostatic hypertrophy), systemic (diabetes, collagen diseases, immune-haematological disorders, neoplasia, neuromuscular disease or surgical sequelae) or anatomical (pyelo-ureteral joint defect) predisposing factors (46 patients), or parenchymal sequelae of previous pyelonephritis (e.g. contracted small-sized kidney due to vesico-ureteral reflux) or renal stones disease (20 patients) were not included in the study.

Complicated APN were excluded to avoid confounding causes in detecting parenchymal inflammatory damage (e.g. an increased pressure in the urinary tract in the obstructive uropathy might alter parenchymal perfusion and consequently either enhancement or diffusion of water molecules).

One of the patients included had a congenital solitary kidney.

Imaging techniques

The diagnosis of pyelonephritis was made by GE-MRI as a second-line imaging technique, used as a gold standard test.

MRI was performed using a 1.5-T system (ACHIEVA, Philips Medical System, The Netherlands) with a maximum gradient strength of 30 mT/m, a slew rate of 150 mT m^{-1} ms^{-1} and a four-channel phased-array coil. As a rule, imaging data were obtained within 48 h of hospitalisation.

Before acquisition of DW-MRI sequences, we performed in each patient a morphological study of the kidneys.

The following protocol was used.

Basal MRI test

- Survey BFFE (balanced fast field echo) sequences along the three orthogonal axes (*x*, *y* and *z*)
- Sequence with function of locator, performed in maximum inspiratory and expiratory breath-hold
- Axial TSE SENSE (turbo spin echo sSSH T2-weighted sequences) (TR=375 ms; double TE=100 ms, Sp 7.0/1.0, turbo factor 47; EPI factor 1, NSA 1, SENSE body coil)
- Axial SPAIR SENSE Sat-SPIR (spectral attenuation inversion recovery) sequences (TR=418 ms; TE=80 ms, Sp 7.0/1.0, turbo factor 47; EPI factor 1, NSA 1, SENSE body coil)
- Axial DWI—TRIG SENSE Sat-SPIR sequences (TR=910 ms; TE=d0.0 72 ms, Sp 7.0/1.0 mm, turbo factor 65; EPI factor 65, NSA 4, matrix 190/256; SENSE body coil; *b* 0-100-700 triggered with imaging time 1.40 min)
- Axial DWI—SENSE Sat-SPIR sequences (TR=1,275–2,572 ms; TE=d0.0 62–65 ms, Sp 7.0/1.0 mm, turbo factor 62–65; EPI factor 62–65, NSA 4, matrix 190/256; SENSE body coil; *b* 0 and *b* 600 with breath-hold and imaging time 20–25 s)

DW MR images with slice thickness of 7 mm and interval of 1 mm were obtained in the axial plane during breath-hold (30 s) by using a single-shot spin-echo EPI (SE EPI) sequence, with three *b* values (0 and 600 s/mm^2). The gradients were applied along the three orthogonal axes (*x*, *y* and *z*) and subsequently averaged to minimise the effects of diffusion anisotropy. The single-shot SE EPI sequence was performed using a parallel imaging technique acquisition (SENSE), which allows a faster acquisition for breath-hold technique and avoids magnetic susceptibility artefacts. Fat saturation was used to prevent chemical shift artefacts, and two presaturation slabs were positioned perpendicular to the anterior and posterior sections, respectively, to suppress motion influences.

- d-ADC maps were then calculated for the different "weightings": *b*=0–600 and *b*=0–100–700. The ADC value was calculated. The mean of the ADC values derived from the regions of interest (ROI=15 mm^2, about 15 pixels) was then calculated in the axial plane. Image analysis was performed off-line at a Windows

workstation (Dell, Xeon CPU 3.20 GHz) with dedicated software (Extended MR WorkSpace 2.6.3.1 2009; Philips Medical Systems, The Netherlands)
- Axial basal WAVE FSAT SENSE (water selective volume excitation) WATS 2D with fat suppression sequences (TR=9.7 ms; TE=4.9 ms; Sp 7.0/3.5 mm, turbo factor 1; EPI factor 1, NSA 1, matrix 128/224; SENSE body coil)

Circular ROIs with a diameter of approximately 1 cm were manually placed in kidney for the measurement of ADC values in the healthy tissue, in the pathological renal parenchyma and in the focal renal lesions. Measurement of the mean ± SD of the ADC values was obtained by three circular ROIs in the mid-kidney at the level of the cortico-medullary junction. For each ROI the average ADC values (ADC_{avg}) were calculated. ADCs of the kidneys were calculated separately for the low (ADC_{low} b=0 s/mm^2) and high (ADC_{high} b=300 or 700 s/mm^2) b values to allow differentiation of the relative influence of the perfusion fraction and true diffusion. Data were processed using Diffusion Analysis software (Extended MR WorkSpace 2.6.3.1 2009).

GE-MRI study

Study after bolus intravenous administration of contrast agent (Gadobutrol, 1 mmol/kg), 2 ml/s:

- Coronal 2D bolus-track sequences (TR=4.0 ms, TE=0.9 ms, Sp 80/0.0 mm, turbo factor 1; EPI factor 1, NSA 1, matrix 128/224; SENSE body coil) in the course of administration of contrast medium with an injector to determine dynamic sequences (care-bolus)
- Coronal Angio-RM 3D RES sequences SENSE, high resolution (TR=5.1 ms, TE=1.5 ms, Sp 3.0/-1.5 mm, turbo factor 1; EPI factor 1; SENSE body coil). After about 20–30 s (cortical-arterial phase). The beginning of MR data acquisition is determined by the vision of the initial opacification of the abdominal aorta using a care-bolus
- Axial dynamic 3D T1-weighted DYN THRIVE (T1 high-resolution isotropic volume examination) sequences—SAT SPIR (fat suppression) (TR=4.0 ms, TE=1.9 ms, turbo factor 60; EPI factor 1, NSA 1, matrix 135/240; SENSE body coil). In the course of administration of contrast medium at 60–80 s (nephrographic phase) and 100–120 s (nephrographic/early excretory phase)
- Axial mdc WAVE FSAT sequences SENSE (water selective volume excitation) WATS 2D with fat suppression (TR=9.7 ms, TE=4.9 ms, Sp 7.0/3.5 mm, turbo factor 1; EPI factor 1, NSA 1, matrix 128/224; SENSE body coil). In late pyelographic phase at 5 min

Analysis of results

When analysing the MRI data, the diagnosis of APN requires demonstration of the following:

- Changes in renal volume (kidney enlargement, presumably due to oedema from active infection)
- Alteration of cortico-medullary delineation (reduced or absent)
- Focal or diffuse parenchymal signal alteration, in the basal test
- After the administration of contrast medium (GE study), on T1-weighted sequences reduction of parenchymal contrast enhancement in the affected area (single or multiple lesions, unilateral or bilateral); presence and size of parenchymal focal lesions; abscessed areas, as fluid lesions delineated by a peripheral halo
- Dilation of the collecting system (mild, moderate, marked)
- Perinephric inflammatory fluid and stranding of the perinephric fat
- Hyperintensity on DW sequences with high b value and hypointensity in the same area on ADC maps, correlating with focal reduction of enhancement at T1-weighted sequences in the GE study (Fig. 1)

Morphological evaluation of the images was performed in consensus by two experienced radiologists who were blinded to the DW-MR images and data. Cortico-medullary delineation and focal or diffuse parenchymal signal alterations, presence and size of parenchymal lesions, dilation of the collecting system and perirenal changes were mainly observed and annotated.

GE-MRI study was finally compared with the DW sequences to evaluate diagnostic agreement, the former being considered the gold standard test.

Considering APN lesions as hyperintense areas due to reduction of water diffusion, sensitivity, specificity, positive and negative predictive value, and overall accuracy of DWI were calculated. Correlation between ADC in normal parenchyma and in pyelonephritic lesions was also statistically analysed.

Results

We recorded 318 patients hospitalised from January 2007 to September 2009 with a clinical diagnosis of APN at ED admission based on the presence of flank pain, fever and leucocytosis or elevated CRP.

MRI was performed in 279 patients (264 female). Morphological examination with GE-MRI was diagnostic in 244 subjects, with evidence of single or multiple areas of parenchymal hypointensity. Thirty-five patients were negative at the GE-MRI examination.

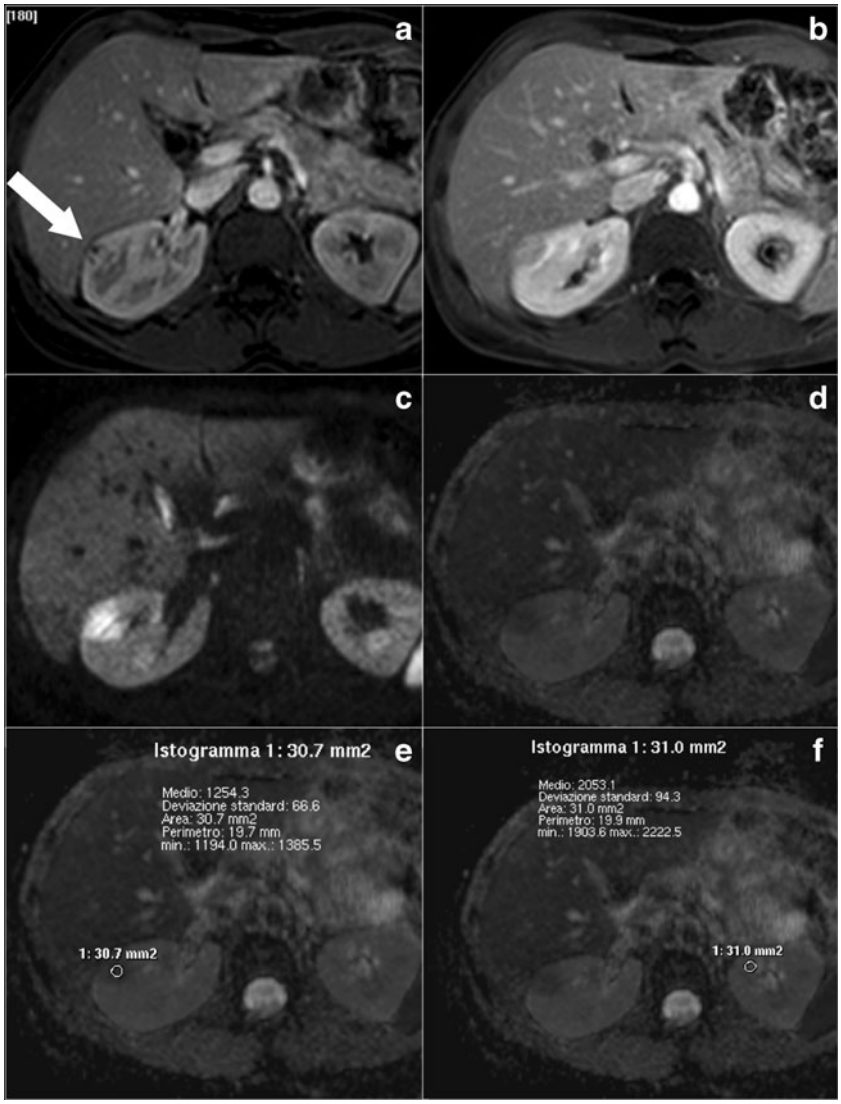

Fig. 1 Acute pyelonephritic lesion in the right kidney. Axial T1-DYN T1 high-resolution isotropic volume examination (THRIVE) imaging after administration of contrast medium in the early (**a**) and nephrographic phase (**b**): heterogeneous defect of contrast enhancement with delimitation of cortical microabscesses (*arrow*). **c** On axial diffusion-weighted imaging sensitivity encoding (SENSE) with $b=700$ s/mm^2, the lesion appears markedly hyperintense. Qualitative apparent diffusion coefficient (ADC) map from diffusion-weighted (DW) echo-planar MR images demonstrates hypointense signal (**d**). The quantitative sampling in the lesion (**e**) and at the level of the middle third of the contralateral parenchyma (**f**) shows significantly lower ADC values in inflammatory parenchymal foci compared with healthy tissue

We included in our study and retrospectively analysed 163 patients with imaging-confirmed diagnosis of non-complicated APN, submitted for both GE-MRI and DW sequences. In keeping with this setting, all patients were female, with a median age of 32 years (16–72 years) and a normal genito-urinary tract.

Four hundred and fourteen MRI examinations were performed, including the first test and the subsequent control investigations (1–4 studies per patient, mean 2.1). GE-MRI was used as a gold standard and confirmed APN in 272 repeated acquisitions (reduced perfusion with enhancement gaps). Among positive studies, DW sequences had a positive result in 258 and a negative result in 14. A radiological confirmation of APN by DW-MRI (parenchymal hyperintensity signal in high *b* images) was obtained in 267 studies (Fig. 1).

Dealing with functional DW-MRI, the mean ADC value was $2.38\pm0.14\times10^{-3}$ mm^2 s^{-1}, with a range of $1.99–2.76\times10^{-3}$ mm^2 s^{-1}. In subjects who underwent repeated MRI, the ADC values were highly reproducible.

Total or sectorial kidney swelling was detected in 121 out of 172 affected kidneys (70.3 %). The severity of the lesion was not uniform. The cortico-medullary gradient was reduced or absent in 18 patients. In 163 patients with onset APN, basal study revealed abnormalities in signal intensity in the foci of inflammation in 65 cases, characterised by a picture of isointensity on T1-weighted sequences and slight hyperintensity on T2-weighted images.

After bolus intravenous administration of contrast agent, about 94.5 % of the patients (154 cases) had lesions in only one kidney. Lesions were bilateral in nine patients (5.5 %), but they were multiple in 128 cases (78,5 %). Overall, 621 lesions were detected, with an average of 3.8 injuries per pathological kidney. Simple non-abscessed lesions only were present in 100 patients, while at least one abscessed lesion was present in 63 patients (38.5 %; Fig. 2) and only 2 had perirenal collections. A thin layer of perirenal effusion was recognised in 104 cases of parenchymal inflammation.

Considering all 414 MR studies, comparing DWI study with GE-MRI used as a gold standard, positive correlation was found in 258 cases (true-positive) and negative correlation in 133 (true-negative). In 14 tests GE acquisitions were positive, while DW sequences were negative (false-negative; Fig. 3). Restriction of the diffusivity of water molecules with slightly hyperintense signal has been highlighted, compared with negative contrast medium enhancement, in nine investigations (false-positive; Fig. 4; Table 1).

Overall DW-MRI versus GE-MRI achieved sensitivity 95.2 %, specificity 94.9 %, positive predictive value (PPV) 96.9 %, negative predictive value (NPV) 92.3 % and diagnostic accuracy (DA) 94.6 % (Table 2).

For a quantitative evaluation, 150 samples of the attenuation coefficient were eventually conducted on the ADC map on parenchymal foci, which always resulted in hypointensity on the map with greyscale; as many comparison samples were collected in areas of healthy ipsilateral parenchyma and in unaffected kidney. In areas of affected parenchyma ADC value in mm^2/s was found to be consistently lower (mean 1.385; minimum 1.109, maximum 1.717; absolute deviation compared with the average 0.150, standard deviation 0.124) compared with healthy parenchyma (mean 2.383; minimum 1.989, maximum 2.763; absolute deviation compared with the average 0.226, standard deviation 0.140), with P value< 0.0001 (Fig. 5).

Discussion

APN is a topic that has remained relatively neglected in terms of imaging research and its diagnosis is still a challenge. None of the clinical signs or laboratory biochemical markers at presentation allows discrimination between a few small lesions and multifocal or abscessed ones [13]. Thus, imaging techniques are needed to assess the severity of kidney involvement and to plan the antibiotic therapy.

Diagnostic imaging plays a role in looking for previous occult structural or functional abnormalities that may require intervention, to assess those patients at significant risk of more life-threatening complications as in diabetic, elderly or immunosuppressed patients, to balance the severity of the infection and to evaluate the extent of organ damage subsequent to a resolved acute infection.

Second-line imaging tests (CT or MRI) should be systematically used to define the presence, extent and type of parenchymal lesions, and to reveal complications (such as abscess or perirenal fluid collections), in order to tailor interventions to the specific clinical contexts [17, 18].

Our interest in APN originated from the observation of the increasing frequency of this disease and from the uncertain indications in the literature with regard to the opportunity to perform DW-MRI [19–23].

Hence, since 2007 we have been collecting data of patients admitted to the ED with a clinical suspicion of APN according to our setting, in order to study the results in non-complicated APN patients routinely hospitalised and undergoing an extensive imaging work-up (ultrasound and either MRI or CT). Our study focused on DW-MRI as an imaging tool for the diagnosis of APN along with treatment and follow-up of patients, also to test the alternatives to our imaging-guided diagnostic and therapeutic approach.

The latest studies have already shown the prospective value of DW-MRI in the assessment of various renal diseases, such as renal ischaemia, pyonephrosis and diffuse renal disease [19–23]. On the contrary, there is no evidence of its role in the diagnosis and follow-up of the APN and no data are available regarding the diagnostic accuracy in adults. Studies conducted in animal models [24] with histological confirmation reported sensitivity and specificity of GE-MRI in the diagnosis of experimentally induced APN,

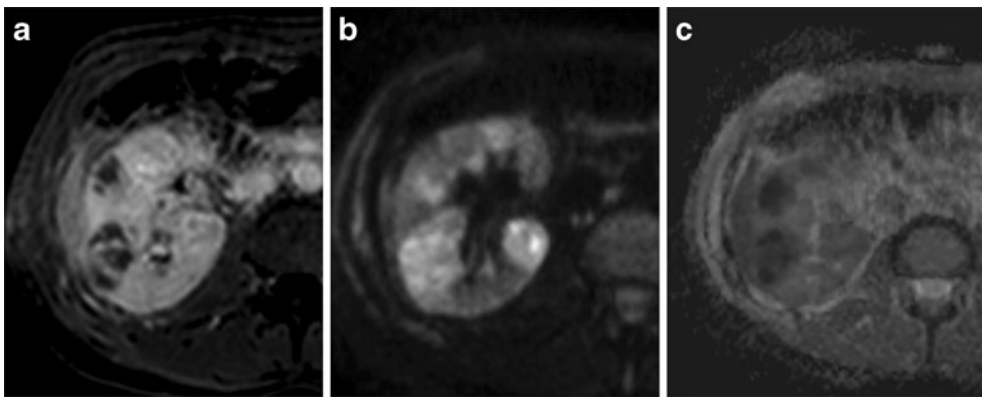

Fig. 2 Severe acute pyelonephritis (APN) with inflammatory parenchymal foci and multiple abscesses. **a** Post-contrast axial T1 water selective volume excitation (WAVE) imaging: the right kidney is swollen and has perfusion defects related to inflammatory parenchymal foci. **b** DWI spin echo (SE) echo-planar image (EPI) with b=700 s/mm^2: lesions appear heterogeneously hyperintense, with small areas of greater intensity due to abscesses. **c** The ADC map shows hypointense signal in correspondence of the same lesions

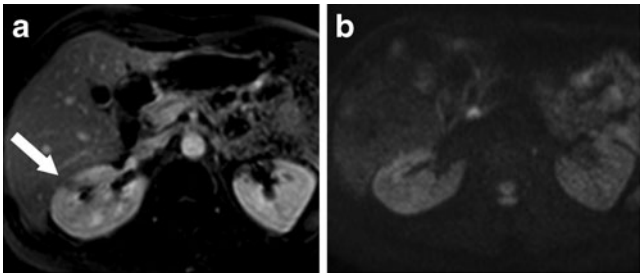

Fig. 3 False-negative DWI study. **a** Small APN lesion in the middle third of the right kidney visible on T1 WAVE sequences after administration of contrast medium in the late nephrographic phase (*arrow*) as an heterogeneous perfusion defect. **b** On DWI sequences the lesion shows no signs of restriction of diffusivity.

respectively, of 91 % and 93 %. Other studies in children, performed in comparison with ^{99m}Tc-DMSA scintigraphy, show that the GE-MRI, using inversion-recovery sequences, has overlapping sensitivity (90.9 %) and specificity (88.8 %) in the diagnosis of APN, but they underline its superiority in differentiating scars from inflammatory foci in the early stages of disease [25].

Gradient echo MRI has a semeiotics and diagnostic accuracy at least comparable to that of CT in the evaluation of morphological and functional impairment in renal inflammation and its complications [26]. Some downsides, however, must be noted. The test is relatively time-consuming (about 20–25 min), with inevitable consequences in the management of the flow of scheduled patients. It also presents high costs and, even if to a lesser extent than iodinated contrast medium, the administration of gadolinium chelates is not recommended in patients with allergic anamnesis. Eventually, studies in recent years on systemic fibrosis due to gadolinium contraindicate its use in patients with renal impairment [27, 28].

In our centre, the study protocol of APN with MRI also implies the use, at baseline, of the DW sequences, with rapid execution. In the literature several investigators suggest the use of DW-MRI in extraneurological fields [29, 30]. In the nephro-urological setting, data of great interest are available in the study of kidney disease, such as chronic impairment

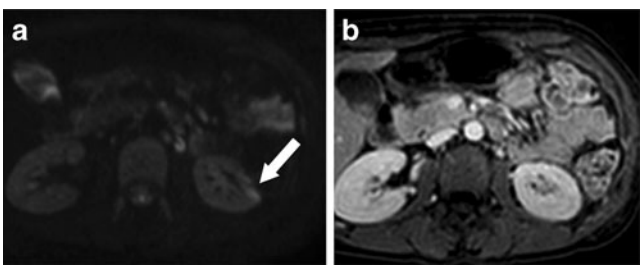

Fig. 4 False-positive DWI study. **a** On axial DWI SENSE with b= 700 s/mm^2 there was a small parenchymal area of restricted diffusion, without enhancement after administration of contrast medium in the T1-WAVE sequence (**b**)

Table 1 Diffusion weighted imaging (DWI) results compared with GE-MRI results

	DW-MRI +	DW-MRI -	
GE-MRI +	258	14	272
GE-MRI −	9	133	142
	267	147	414

or infections [19–22, 31], dealing with the characterisation of focal lesions [32–34], in the definition of renal function [23] and follow-up in the renal transplant setting [35]. Recently, Taouli et al. [36] and Kim et al. [37] were the first to compare DW-MRI with GE-MRI, emphasising the value of DW sequences, able not only to add valuable diagnostic information but also to be considered a valid alternative to contrastographic investigation in the characterisation of focal renal lesions.

As shown by the results of our study, comparing the diagnostic accuracy of DW sequence with contrast-enhanced MRI, DW-MRI clearly has high sensitivity, specificity, positive/negative predictive value and diagnostic accuracy, all close to 95 %.

The evaluation of the data detected a very small number of false-positives (FP) and false-negatives (FN), moreover based on images of very small extension and found in tests carried out in the monitoring phase. In particular, FN were represented by areas of irregular parenchymal contrast medium enhancement and absence of signal abnormalities on DW-MRI. In these cases there might be the onset of inflammatory foci on a background of parenchymal scarring due to previous infection: once the acute injury resolved, it remains a contrast enhancement caused by pre-existing parenchymal distortion. Another explanation for these events could be that the inflammatory lesions had been already improved when the patients were submitted for radiological examination or that they were so mild as to be undetectable. The FP, in turn, corresponded to focal parenchymal hyperintensity on DW-MRI without correlated enhancement after administration of gadolinium. This framework, as well as being secondary to artefacts, dealing with the extreme sensitivity of the DW-MRI to movement, can be related to the phenomenon of persistence of the T2 signal, even with high b values, referred to as “T2 shine-through”, which occurs in

Table 2 Diagnostic performance of DW-MRI versus GE-MRI

Sensitivity	95.2 %
Specificity	94.9 %
Positive predictive value	96.9 %
Negative predictive value	92.3 %
Diagnostic accuracy	94.6 %

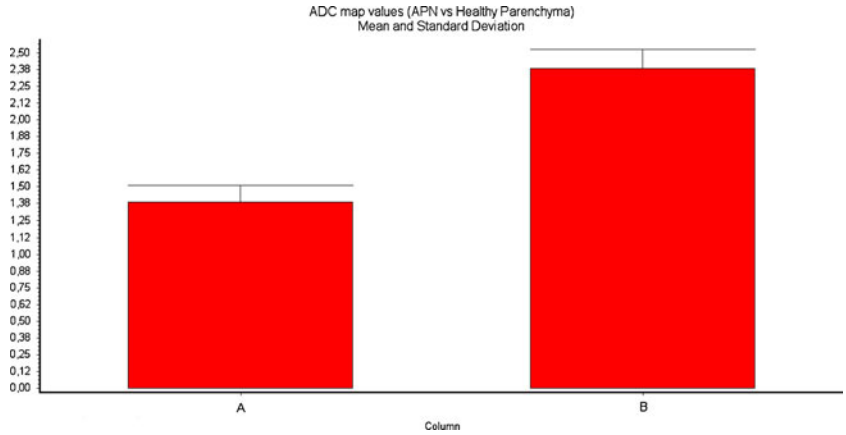

Fig. 5 Mean (± SD) of the ADC map values in a sample of 150 lesions, measured in the APN foci (*column A*) and in the contralateral healthy corresponding parenchyma (*column B*). The difference between the two values (1.385±0.124 vs 2.383±0.140) was extremely significant ($P<0.0001$)

tissues where there is a free diffusion of water molecules. This finding, presumably detectable in the presence of small residual collections or microcysts, leads to mistakes in the qualitative assessment of DW images, which require verification with the study of the ADC map. Finally, it may be assumed that the weakly hyperintense signal only detectable on DW-MRI may be related to persistent moderate inflammatory events of such magnitude as to go undetected by contrast enhanced testing, assuming the more sensitive evaluation by DW-MRI. The phenomenon, which occurred invariably in subsequent controls in areas where in the acute phase there was a more marked inflammatory process, may suggest that the gold standard tends to underestimate the process and that DW-MRI allows a greater "conspicuity" than contrast-enhanced examination. This finding, which to our knowledge does not find any other description in the literature and that is probably secondary to minor compressive alterations due to a residual component of oedematous swelling, together with slight irregularities in the tissue microperfusion (so-called "pseudodiffusion"), should find histological confirmation, but this is not feasible in an abnormality without surgical implications. However, in clinical practice, in case of persistent positivity of DW-MRI after the negativity of the clinical setting and the completion of the programmed therapy, the finding must be considered not relevant and the patient recovered.

Because of the inflammatory parenchymal damage responsible for interstitial space reduction, with a resulting decrease in the diffusivity of water molecules, the quantitative evaluation of the ADC map is of considerable importance. It is based on the study of the ADC of water molecules, always associated with qualitative analysis of the DW signal, to avoid mistakes related to the influence of T2 weighting of the sequence. In selected subjects with a proper clinical laboratory grading, it was interesting to note how the inflammatory disease could be identified not only on the basis of the hyperintense signal on DW-MRI, with high *b* factor and with hypointensity on the ADC map, but also as a result of a calculation of the attenuation coefficient after ROI positioning, with the lowest result compared with that obtained on areas of healthy parenchyma at the corticomedullary junction [38]. The results derived from estimates, especially for lesions of limited dimensions, still encounter uncertainties because of the choice of the "*b*" factor, for the inter-operator variability in measuring with ROI ADC values of some specific areas, as well as on the possible differences between the magnets (either from different manufacturers or because of different field strengths of devices of the same company) [38, 39]. This aspect is a significant problem that has not been solved; indeed, several authors using different *b* values have not come to superimposable results [40]. In agreement with data reported by Macarini et al. [38], with reduced acquisition times, the value of the "*b*" factor of approximately 600–700 used in our study can be considered an acceptable compromise between image quality, affected by a high "*b*", which reduces the signal-to-noise ratio (SNR), and a weighting of the "real" diffusion that is more faithful and true with these values. As recommended by Fukuda et al. [41], the ROI cursors were placed at the level of the middle third of the kidney in correspondence with the cortico-medullary junction, as the evaluation of ADC values in the central portion of the kidneys is less influenced by the perfusion effect. With such a procedure it is more reliable to make a comparison with data derived from the positioning of the ROI in inflammatory parenchymal foci [21].

Different studies [23, 31, 32, 38, 42] have calculated the intrinsic proton diffusion in the abdominal organs and, in particular, in the kidneys. In the literature the normal reported values range from 1.60 to 2.65×10^{-3} mm^2 s^{-1}, probably in relation to the breadth of the diffusion gradient used (500–1,300 s/mm^2). According to data in the literature, in our study the mean value of renal parenchyma in healthy subjects was $2.40\pm0.20\times10^{-3}$ mm^2 s^{-1}. Comparing our study on APN with other results, Thoeny et al. [21] studied a population of healthy volunteers and patients with various

parenchymal diseases; in the APN patients they found ADC values of entities significantly lower than in healthy contralateral parenchyma, showing one of the few reports where reference is made precisely to inflammatory renal parenchymal disease and in which the results have been very similar to ours.

In conclusion, according to our study results, DW-MRI of the kidney seems to be a feasible, rapid and reliable method as quantification of ADC values can be useful in diagnosing non-complicated APN. The high diagnostic agreement we have found between GE-MRI and DW-MRI offers new perspectives in diagnostic management, enabling monitoring of APN in a short time without use of ionising radiation or administration of paramagnetic contrast medium. We can assume the use of DW-MRI, together with the performance of the usual basal sequences T1 and T2, in the acute phase, possibly in the ED, affecting minimally (negligible time is required) the workflow of the MRI service, thus allowing a timely therapeutic approach. The subsequent checks, performed about every 3 weeks until complete resolution of the inflammatory process, may instead be programmed with DWI alone.

In addition, DW-MRI is an alternative to dynamic investigation in all cases where there are contraindications to administration of iodinated and/or paramagnetic contrast medium, such as those patients with renal insufficiency and pregnant or lactating women. Eventually, the short duration of the examination and the easy response and reproducibility of ADC values allow a proper diagnostic evaluation even in uncooperative subjects or slightly sedated claustrophobic ones.

Dealing with costs too, DW-MRI is an interesting tool for detecting non-complicated APN, thanks to its inherent cost and its potential impact on the suitability and timeliness of treatment.

References

1. Hooton TM, Stamm WE (1997) Diagnosis and treatment of uncomplicated urinary tract infection. Infect Dis Clin North Am 11:551–581
2. Georgi A, Reddy YNV, Gautam G (2012) Diagnosis of acute pyelonephritis with recent trends in management. Nephrol Dial Transplant 27:3391–3394
3. Ramakrishnan K, Schedi DC (2005) Diagnosis and management of acute pyelonephritis in adults. Am Fam Physician 71:933–942
4. Medical Research Council Bacteriuria Committee (1979) Recommended terminology of urinary tract infection: a report by the members of Medical Research Council Bacteriuria Committee. Br Med J 2:717–719
5. Talner LB, Davidson AJ, Lebowitz RL, Dalla Palma L, Goldman SM (1994) Acute pyelonephritis: can we agree on terminology? Radiology 192:297–305
6. Dyer RB (1997) CT of renal inflammatory disease. Invited commentary. Radiographics 17:867–868
7. Soulen MC, Fishman EK, Goldman SM, Gatewood OM (1989) Sequelae of acute renal infection: CT evaluation. Radiology 173:423–426
8. Webb JAW (1987) The role of imaging in adult acute urinary tract infection. Eur Radiol 7:837–843
9. Gupta K, Hooton TM, Naber KG et al (2011) International clinical practice guidelines for the treatment of acute uncomplicated cystitis and pyelonephritis in women: a 2010 update by the Infectious Diseases Society of America and the European Society for Microbiology and Infectious Diseases. Clin Infect Dis 52:103–120
10. Parenti GC, Passari A (2001) Pielonefrite acuta: ruolo della diagnostica per immagini. Radiol Med 101:251–254
11. Craig WD, Brent JW, Travis MD (2008) From the archives of the AFIP, pyelonephritis: radiologic-pathologic review. Radiographics 28:255–276
12. Majd M, Nussbaum Blask AR, Markle BM et al (2001) Acute pyelonephritis: comparison of diagnosis with 99mTc-DMSA, SPECT, spiral CT, MR imaging, and power Doppler US in an experimental pig model. Radiology 218:101–108
13. Piccoli GB, Consiglio V, Deagostini MC et al (2011) The clinical and imaging presentation of acute "non complicated" pyelonephritis, a new profile for an ancient disease. BMC Nephrol 12:68–78
14. Martina MC, Campanino PP, Caraffo F et al (2010) Dynamic magnetic resonance imaging in acute pyelonephritis. Radiol Med 115:287–300
15. Nikken JJ, Krestin GP (2007) MRI of the Kidney: state of the art. Eur Radiol 17:2780–2793
16. Hagmann P, Jonasson L, Maeder P, Thiran JP, Wedeen VJ, Meuli R (2006) Understanding diffusion MR imaging technique. Radiographics 26:S205–S223
17. Kawashima A, Sandler CM, Goldman SM (2000) Imaging in acute renal infection. BJU Int 86:70–79
18. Johansen TE (2004) The role of imaging in urinary tract infections. World J Urol 22:392–398
19. Muller MF, Prasad PV, Bimmler D, Kaiser A, Edelman RR (1994) Functional imaging of the kidney by means of measurement of the apparent diffusion coefficient. Radiology 193:711–715
20. Chow LC, Bammer R, Moseley ME, Sommer FG (2003) Single breath-hold diffusion-weighted imaging of the abdomen. J Magn Reson Imaging 18:377–382
21. Thoeny HC, De Keyzer F, Oyen RH, Peeters RR (2005) Diffusion-weighted MR imaging of kidneys in healthy volunteers and patients with parenchymal diseases: initial experience. Radiology 235:911–917
22. Xu Y, Wang X, Jiang X (2007) Relationship between the renal apparent diffusion coefficient and glomerular filtration rate: preliminary experience. J Magn Reson Imaging 26:678–681
23. Carbone SF, Gaggioli E, Ricci V, Mazzei F, Mazzei MA, Volterrani L (2007) Diffusion-weighted magnetic resonance imaging in the evaluation of renal function: a preliminary study. Radiol Med 112:1201–1210
24. Pennigton DJ, Lonergan GJ, Flack CE, Waguespeck RL, Jackson CB (1996) Experimental pyelonephritis in piglets: diagnosis with MR imaging. Radiology 201:199–205
25. Kovanlikaya A, Okkay N, Cakmakci H, Ozdoðan O, Degirmenci B, Kavukcu S (2004) Comparison of MRI and renal cortical scintigraphy findings in childhood acute pyelonephritis: preliminary experience. Eur J Radiol 49:76–80
26. Israel GM (2006) MRI of the kidney and urinary tract. J Magn Reson Imaging 24:725–734
27. SIRM-SIN-AINR (2007) Fibrosi nefrogenica sistemica. Raccomandazioni per l'uso degli agenti di contrasto a base di Gadolinio. http://www.sirm.org e www.sin-italy.org. Accessed 30.10.2007

28. Sadowski EA, Bennett LD, Chan MR et al (2007) Nephrogenic systemic fibrosis: risk factors and incidence estimation. Radiology 243:148–157
29. Arlinghaus LR, Li X, Levy M et al (2010) Current and future trends in magnetic resonance imaging assessments of the response of breast tumors to neoadjuvant chemotherapy. J Oncol 2010
30. Eccles CL, Haider EA, Haider MA, Fung S, Lockwood G, Dawson LA (2009) Change in diffusion weighted MRI during liver cancer radiotherapy: preliminary observations. Acta Oncol 48:1034–1043
31. Namimoto T, Yamashita Y, Mitsuzaki K, Nakayama Y, Tang Y, Takahashi M (1999) Measurement of the apparent diffusion coefficient in diffuse renal disease by diffusion weighted echo-planar MR imaging. J Magn Reson Imaging 9:832–837
32. Cova M, Squillaci E, Stacul F et al (2004) Diffusion-weighted MRI in the evaluation of renal lesions: preliminary results. Br J Radiol 77:851–857
33. Squillaci E, Manenti G, Di Stefano F, Miano R, Strigari L, Simonetti G (2004) Diffusion-weighted MR imaging in the evaluation of renal tumours. J Exp Clin Cancer Res 23:39–45
34. Zhang J, Tehrani YM, Wang L, Ishill NM, Schwartz LH, Hricak H (2008) Renal masses: characterization with diffusion-weighted MR imaging-a preliminary experience. Radiology 247:458–464
35. Palmucci S, Mauro LA, Veroux P et al (2011) Magnetic resonance with diffusion-weighted imaging in the evaluation of transplanted kidneys: preliminary findings. Transplant Proc 43:960–966
36. Taouli B, Thakur R, Mannelli L et al (2009) Renal lesions: characterization with diffusion-weighted imaging versus contrast-enhanced MR imaging. Radiology 251:398–407
37. Kim S, Jain M, Harris AB et al (2009) T1 Hyperintense renal lesions: characterization with diffusion weighted MR imaging versus contrast-enhanced MR imaging. Radiology 251:796–807
38. Macarini L, Stoppino LP, Milillo P, Ciuffreda P, Fortunato F, Vinci R (2010) Diffusion-weighted MRI with parallel imaging technique: apparent diffusion coefficient determination in normal kidneys and in non malignant renal diseases. Clin Imaging 34:432–440
39. Colagrande S, Belli G, Politi LS, Mannelli L, Pasquinelli F, Villari N (2008) The influence of diffusion and relaxation-related factors on signal intensity: an introductive guide to magnetic resonance diffusion-weighted imaging studies. J Comput Assist Tomogr 32:463–474
40. Colagrande S, Carbone SF, Carusi LM, Cova M, Villari N (2006) Magnetic resonance diffusion-weighted imaging: extraneurological applications. Radiol Med 111:392–419
41. Fukuda Y, Ohashi I, Hanafusa K et al (2000) Anisotropic diffusion in kidney: apparent diffusion coefficient measurements for clinical use. J Magn Reson Imaging 11:156–160
42. Mürtz P, Flacke S, Träber F, Van den Brink JS, Gieseke J, Schild HH (2002) Abdomen: diffusion-weighted MR imaging with pulse-triggered single-shot sequences. Radiology 224:258–264